Impact of Chemically Synthesized Iron Oxide Nanoparticles with/without Magnesium Nanoparticles on Iron Deficiency Anemia *in vivo*

Rania Ahmed S.M. [a,b], Abdel Moneam M.N.[b], Abdel Kader A.S.[b], Hanaa H. El-Sayed[c]

[a] *Food Science Department, National Nutrition Institute, 11562 Cairo, Egypt*
b biochemistry department, Faculty of Agriculture, Cairo Giza 12613, Egypt
[c] *Nutritional Chemistry and Metabolism Department, National Nutrition Institute, 11562 Cairo, Egypt*

Iron oxide nanoparticles were used in earlier searches to treat iron deficiency anemia; this search applied magnesium nanoparticles with iron to know what the occurrence is.

Abstract

Iron deficiency anemia (IDA) is a significant global public health issue. Herein, chemically synthesized iron oxide magnetic nanoparticles (IONPs) and magnesium oxide nanoparticles (MgO-NPs) were characterized and evaluated as treatments for IDA. For *in vivo* assessment, fifty Sprague-Dawley rats were divided into 5 groups: negative group, positive control or anemic rats, and four treated sets with different iron formulations (n = 10). IDA was induced by feeding rats a Fe-deficient diet, after which they were treated orally with different iron compounds for 4 weeks. Biological and hematological parameters were followed up during the treatment period. Results demonstrated that all examined groups had a positive curing impact, attaining normal values, while FeMgO-NPs exhibited the highest results in bioavailability (HRE ratio/day% and RBV HRE ratio/day %), hematological parameters, and transferrin saturation% among examined groups. Additionally, the histopathological structures revealed that the damage in the liver tissues of anemic rats persisted after feeding on $FeSO_4$ and IONPs, except that FeMgO-NPs were better. While the spleen was normal in all repleted groups. This demonstrates that iron bioavailability rises when IONPs are used therapeutically to treat IDA, returning it to normal levels. However, it must be supported by other metals to increase its properties and minimize its adverse effects.

Keywords: iron deficiency anemia – fortification – IONPs - MgO-NPs

DOI: 10.48047/ecb/2022.11.12.114

Introduction

Iron deficiency anemia (IDA) is an essential worldwide health epidemic [1]. The prevalence of anemia in the world in 2019 was 39.8% in children aged 6 to 59 months, 29.6% in non-pregnant women, and 36.5% in pregnant women [2]. While 25% of women were anemic, according to The Demographic and Health Survey of Egypt (2014) [3]. Women in rural Upper Egypt had the highest anemia rate (31%). Anemia is a blood condition characterized by a lack of sufficient RBC mass to adequately oxygenate peripheral tissues [4-7] and according to WHO, 2011 anemia is defined as a g/L level of less than 120 in non-pregnant adult women and less than 110 in pregnant women [8]. Malnutrition, iron shortage in diet, insufficient iron absorption, and excessive iron absorption by the placenta

or fetus are the main causes of IDA, which happens when the synthesis of hemoglobin and iron-containing enzymes is inhibited by iron [9].

Iron is an essential trace element for sustaining basic cellular functions and promoting immunity in response to infections and immunizations. It also participates in numerous enzyme systems in the body and is necessary for oxygen transport [10, 11]. The most straightforward method of broadly and sustainably increasing iron intake is frequently through food fortification. It is one of the most economically advantageous global development initiatives [12]. The British Society of Gastroenterology advises using ferrous preparations, particularly ferrous sulphate, as the first line of treatment for iron depletion because they are affordable, have high bioavailability, are readily available in a variety of forms, and have been proven to effectively replenish iron stores and treat anemia [13]. However, there are also many limitations to their use, with the most common being the frequency and severity of side effects.

Due to their physiochemical characteristics and small particle size (1-100 nm), magnetic nanoparticles (NPs) are receiving more interest in nanoscience and nanotechnology [14]. The solubility and in vivo bioavailability of iron compounds are increased to the level of $FeSO_4$ without interacting with the food matrix by significantly increasing their specific surface area (SSA) about mass when reduced to the nanoscale [15-17]. Several authors have looked into the use of nanoparticles (NPs) as dietary supplements over the past few years They have used magnetic iron NPs [18], oxide iron NPs [16,19,20] or iron phosphate NPs [15,21,22] they use nano iron supplements, iron hydroxide adipate tartrate (IHAT), to treat IDA in young children. The coprecipitation approach is commonly used as a straightforward procedure for producing inorganic and metal-based nanoparticles. Iron oxide nanoparticles are frequently produced by the coprecipitation technique and are well-known in the biomedical field for numerous benefits. This technique has many advantages, including great product yield, eco-friendly solvent, and limited size dispersion. the species that often dissolves in aqueous solutions to generate the particles [23].

Huang et al. [24] found a clear correlation between magnesium deficiency and a higher frequency of anemia, especially in elderly women. Magnesium is necessary for the hematopoietic system [25]. In the US, it is common to fall short of the recommended daily magnesium intake, and 28% of pregnant women have anemia as a result [26]. According to a cross-sectional retrospective study by Zeynep et al. [27], anemia among persons with chronic renal disease is positively associated with magnesium deficiency. Cinar et al. [28] found that magnesium supplementation also increases athletes' hemoglobin levels. The relationship between dietary magnesium intake and anemia in the general population is poorly understood. [24]

Aim of study

This research studied the impact of iron and magnesium oxide nanoparticles, which were chemically synthesized, via a coprecipitation method, characterized in terms of structural, morphological, and dimensional properties using X-ray diffractometry (XRD), transmission electron microscopy (TEM) imaging, Fourier transform infrared (FTIR)

spectroscopy and finally studied its biological and histopathological effect when used as food fortificants to alleviate iron deficiency symptoms in vivo.

Material& methods

Nanoparticles Materials Synthesis

All chemicals were of analytical reagent grade and were used without further purification

Preparation of IONPs

Magnetite iron oxide Fe_3O_4 nanoparticles were created using the co-precipitation process, as described in [29]. Briefly, 20 ml of aqueous (1 M $FeCl_3$ hexahydrate) solution and 5 ml of aqueous (2 M $FeSO_4$ heptahydrate in 2 M HCl) solution were added dropwise to 250 ml of 0.7 M ammonia solution in deoxygenated surroundings by bubbling N2 gas until the color of the reaction mixture turned to black. The mixture was then stirred and sonicated for 30 minutes. The precipitate was recovered using a magnetic field, washed three times with deionized water, and centrifuged to separate the sediment. The precipitate was then ground after being dried at 60 °C.

Precursor agent → Reducing agent

$$\text{Reducing agent} + Fe^{3+} \rightarrow Fe^{2+} + \text{By} - \text{products}$$

$$Fe^{2+} + Fe^{3+} + 8OH^- \rightarrow Fe_3O_4 + 4H_2O$$

Preparation of FeMgO-NPs.

Magnesium oxide (MgO) nanoparticles were synthesized according to Wahab, et al., [30] method which is based on the dissolving of 0.2 M Magnesium nitrate ($MgNO_3$ $6H_2O$) in 100 ml of deionized water and then adding a drop wisely to a solution of 0.5M sodium hydroxide under continue stirring for 30 min until white precipitate of magnesium hydroxide appeared. PH was adjusted to 12.5. The precipitate was filtered and washed three times with methanol to remove ionic impurities then centrifuged at 5000 rpm/min for 5 min and dried at Room temperature. The dried precipitate was calcinated in the furnace at 300 °c for 2h. Iron / Mg oxides mixture was prepared by mixing iron oxide nanoparticles as magnetite Fe3O4 with MgO nanoparticles in a ratio of 1:2.

Chemical and structural characterization:

Imaging, Particle size, and morphological features of nanoparticles were determined by using a High-resolution Transmission Electron Microscope (HR-TEM, Tecnai G20, FEI, and Netherland) Two different modes of imaging were employed; the bright field at electron accelerating voltage 200 kV using lanthanum hexaboride (LaB6) electron source gun and the diffraction pattern imaging. An Eagle CCD camera with (4k*4k) image resolution was used to acquire and collect transmitted electron images. TEM Imaging & Analysis (TIA) software was used for spectrum acquisition and analysis of EDX peaks. XRD diffraction was measured using an X-ray diffractometer (X, PERT – PRO – PANalytical – Netherland, CuKα radiation 45KV, 30mA, and k=1.54060 A°). The optical properties of nanoparticles

were analyzed via UV-VIS spectrophotometer (Cary 500, UV-VIS- NIR spectrophotometer) in a wavelength range of 175-3300 nm. The functional group of the synthesized nanoparticles was characterized by the Fourier Trans – Form infrared (FTIR) spectroscopy (Compaq, FT/IR -6100 TypeA) with a frequency range from 4000 to 400 Cm^{-1}. The stochiometric composition of nanoparticles was analyzed by inductively coupled plasma (ICP MS/MS 8800 Triple Quad - Agilent Technologies) [31].

In vivo experiment

Ethical approval for animal study. All experiments were approved by the National Hepatology and Tropical Medicine Research Institute (serial: A4)

Experimental animals

50 female Sprague Dawley rats (21 days old, initial body weight 60±10 g) obtained from Vaccine and Immunity Organization, Helwan Farm, Cairo, Egypt were housed individually in stainless steel cages with wire mesh floors and kept under controlled conditions (room temp 21°c and 50-60% humidity) with a daily 12h/12h light/dark cycle. Food and double distilled water were provided *ad libitum.* Animals received humane care in compliance with the institution's guidelines in the experimental laboratory animal, Department of Nutrition Chemistry and Metabolism, National Nutritional Institute.

Experimental diets:

Diets were prepared based on the nutritional needs of animals according to AIN -93 G rodent diets [31] with some modifications. Normal (negative control) fed a normal basal diet (Fe content: 35 mg/Kg diet) for 4 weeks. Iron deficiency anemia was induced in the remained rats (40 rats) by feeding with a Fe-deficient diet (Fe-free diet with Zn content as 0.2%) according to Yanagisawa et al., [33] and Yanagisawa et al. [34] until rats had an average HB concentration of ≤10 g/dl [35]. At the end of the depletion period, (8 weeks) rats were randomly assigned to 4 groups that consumed a Fe-deficient diet as follows: Group (1): served as the positive control group (received no treatment) and consumed a Fe-deficient diet for 4 weeks. Group (2): served as an anemic group treated with $FeSO_4$ (Fe con 35mg/Kg diet). Group (3): served as an anemic group treated with a 20mg /kg diet of IONPs. Set 4) served as an anemic group treated with a 20mg /kg diet of FeMgO-NPs.

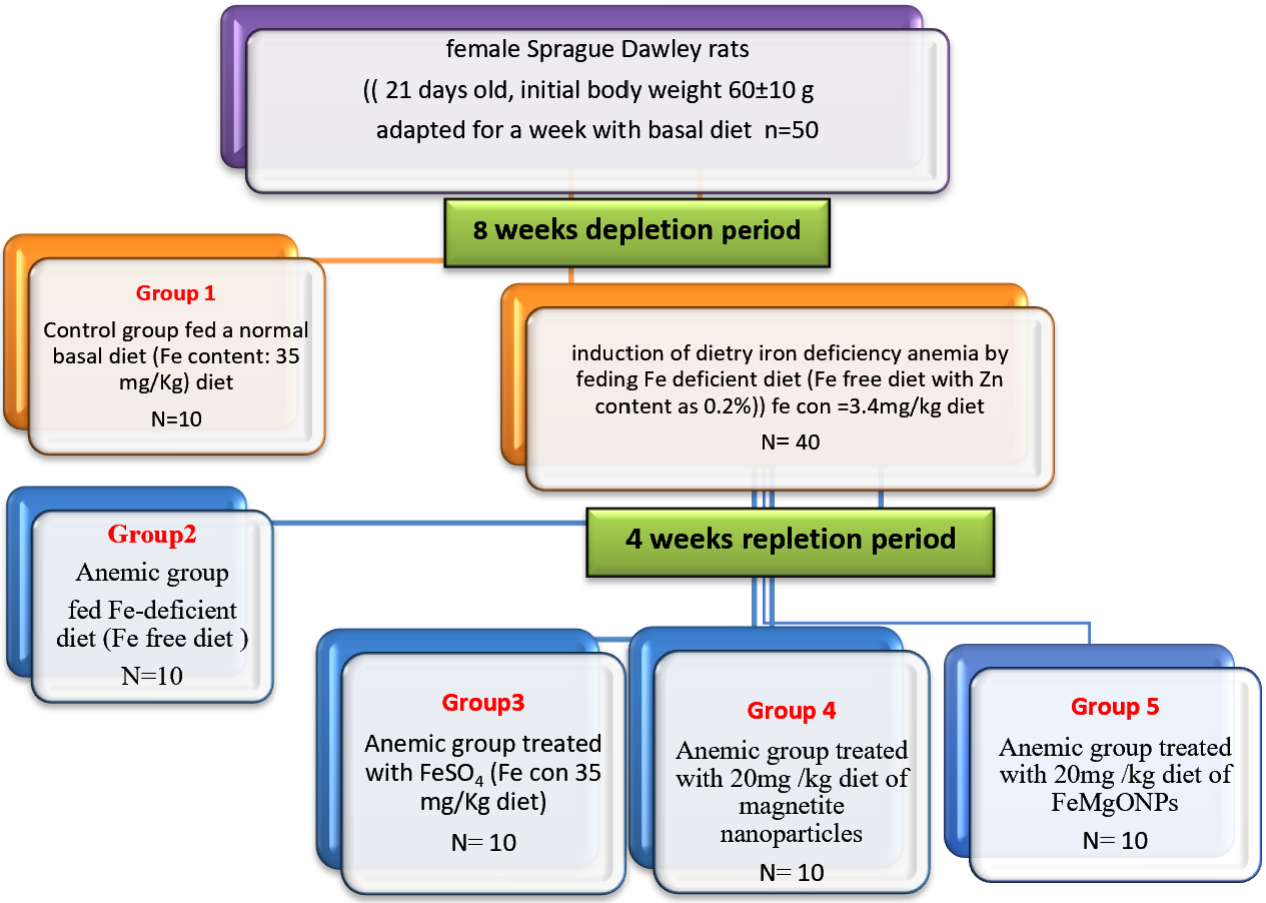

Figure 1 /Schematic representation of Experimental design for iron repletion with nanostructured compoundsin rats.

Laboratory analysis:

Blood collection and handling:

Blood was drawn from the orbital venous plexus [36] under diethyl ether anesthesia through heparin-coated capillaries into an EDTA-coated capillary tube for immediate hematological parameters determination.

Biological parameters:

Feed intake and body weight gain (BWG): Individual food consumption and body weight were weighed once a week throughout the experiment. Body weight gain, [37] and Feed efficiency ratio (FER) were calculated according to [38].

Bioavailability indices calculations

Initial and final body weight, initial and final Hb concentrations, and the amount of Fe consumed during the repletion period and post-repletion period (normal basal diet) for each animal were used to estimate the following variables:

a)-The efficiency percentage of the conversion of food iron into hemoglobin can be calculated as hemoglobin regeneration efficiency (HRE) according to [39,40]

HRE = [Final Hb Fe (mg) - Initial Hb Fe (mg)] / Fe consumed (mg)

b– Iron content of Hb: calculated according to Eggum, [38] and Mahoney and HENDRICKS [39] by assuming that 6.7% of the rat's body weight is blood and Hb contains 0.335% (w/w) iron.

Initial Hb Fe (mg) = Initial BW (g) x 0.067ml/g BW x Initial Hb g/100ml x 3.35 mg Fe / g Hb

Final Hb Fe (mg) = Initial BW (g) x 0.067ml/g BW x Initial Hb g/100ml x 3.35 mg Fe / g Hb

c-The relative Fe bioavailability was calculated by dividing the individual HRE values of Fe sources by the mean HRE value of ferrous sulfate according to [39, 41]

RBV_{HRE} ratio = (HRE test diet each animal / HRE from $FeSO_4$ diet)

Where BW = body weight, Hb = hemoglobin

Hematological parameters

Complete blood count (CBC) analyses were determined in all rats before the beginning of the experiment to ensure that values were statistically non-significant between all the experimental groups ($P > 0.05$). Then measurements were done in rats in all groups every 2 weeks during the experiment by using (Diagon D-Cell 60 Hematology Analyzer) at the blood analysis unit in the National Nutritional Institute.

Blood iron saturation analysis and liver iron concentration

Serum iron [42], Total iron binding capacity was measured according to Piccardi et al., [43]. The iron concentration of samples was measured by inductively coupled plasma emission spectrometry by inductively coupled plasma (ICP MS/MS 8800 Triple Quad-Agilent Technologies) according to Parker [31]

Histological examination of tissues:

Histological examination of tissues was performed in Cairo University, faculty of veterinary medicine as follows: Liver and spleen tissues, which were immersed in 10% of neural buffered formalin, dehydrated with xylene, and descending alcohol row. Tissues then embedded in paraffin and sections 4-5 Mm thick were cut from the paraffin blocks and stained with hematoxylin – Eosin for histological examination [44]. Perls' Prussian blue was used to detect the presence of iron.

Statistical analysis

Descriptive statistics of the data were performed by Microsoft Excel 2010, and the data were represented as mean ± SEM. Statistical analyses were performed using SPSS 22.0 software. Rat body weights and their hematologic and biochemical data were analyzed using one-way ANOVA followed by the Tukey test. The P-values of less than 0.05 were considered statistically significant. [45]

Result and Discussion

Characterization of particles

TEM analysis

As depicted in Fig. 2 (A), the mean diameter of iron oxide nanoparticles was evaluated using transmission electron microscopy (TEM; Philips CM 10, Eindhoven, The Netherlands). Iron oxide nanoparticles appear to have homogenously spherical nanoparticles with an average diameter of 10 nm, in the form of nanoparticle agglomerates. This result is consistent with some previous investigations [46]. However, MgO-NPs have a spherical-shaped nanoparticle with an average diameter of 28.15 nm. [47,48]. The produced formulations' size is between 10 and 100 nm, which allows them to bypass the reticular endothelial system (RES) and prolong their blood circulation period. [49].

XRD analysis

Dried Fe_3O_4 NPs were first characterized in terms of crystal structure, size, and shape. The XRD pattern for Fe_3O_4 NPs is shown in Fig. 2 (C) revealing a crystalline phase with main diffraction peaks indexed as (220), (311), (400), (511), and (440), such as for the cubic spinel structure of Fe_3O_4 (ICDD PDF card no. 04-006-6550) enables to confirm the Fe_3O_4 composition and to exclude the presence of Fe_2O_3 phase, as its characteristic extra peaks (around 15, 24, and 26°) are not observable. This result is in agreement with [45-50]. However, the diffraction patterns of MgO-NPs demonstrated peaks at 2θ of 36.86, 42.82, 62.17, 74.5,2, and 78.44 º were associated with (111), (200), (220), (311), and (222) respectively (ICDD PDF card no . 04-007-3846). This result was matched by Abbas, and Adim [47]; Abinaya and Kavitha [48]; Subash, et al., [53]; and Ameur et al., [54].

FTIR analysis

As shown in Figure 2 (D), the FTIR spectra of the magnetite showed the characteristic vibrations of the Fe–O bonds of the magnetite at around 624 to 425 cm−1. Typically, peaks observed below 1000 cm−1 in spinel ferromagnetic, attributed to metal-oxygen bonds, absorption bands Fe-O at 566.96 cm−1, 421.37 cm−1in magnetite spectra are observed corresponding to the intrinsic stretching vibrations of metal-oxygen at the tetrahedral site (Fe tetra-O) and at the octahedral site (Fe octa–O), respectively. Moreover, the band at 1622 cm−1 is due to water molecules adsorbed on the magnetite surface. The characteristic O–H bending vibrations are indicated by the bands at 3372.89 cm-1. This results in agreement with Ameur et al., [54]. After adsorption, there is a slight shift in the band centered at 567 cm−1, corresponding to the Fe–O bonds. In addition, The OH group presence in both forms is marked as a broad absorption above 3200 cm−1. The bending

vibrations of the adsorbed water molecules on the surface of nano-forms appeared at ~1623 cm−1, [45, 50] the bands attributed to SO4- were observed at 1110.8 cm-1 in nano-form. Results are in agreement with Li et al., [56]; and Zhang et al., [57].

The micrographs of the sol-gel contain a broad peak at 3449 cm^{-1}, which is also caused by the presence of the OH molecule, which is necessary for the synthesis of MgO NPs from their precursor, [48, and 58]. As well as by the N-H bending of the amine bond. The primary amine (N-H) bending mode overlapped with either an amide or carboxylate salt is represented by the medium peak measured at 1654 cm−1. [48]. Additionally, the observed band in the range of 1560cm-1 is attributed to the N-H bending vibrations, and the significant peaks in the region of 1370 cm^{-1} are linked to the bending vibration of CH2 groups. The cubic structure of MgO was shown by the observation of an absorption band close to the point of 862 cm-1. [59, 60].

UV-VIS spectral analysis

Fig. 2 (B) exhibited the characteristic peaks of magnetite nanoparticles at 370 nm by using a UV-VIS spectrophotometer. [61, 62] While λmax of MgO-NPs was 225 nm this result was in agreement with Subash, et al. [53] and Todan, Ligia, et al. [63] Who mentioned that the maximum absorption band was assigned to the excitation of five coordinated oxygen anions from the periclase structure of MgO-NPs.

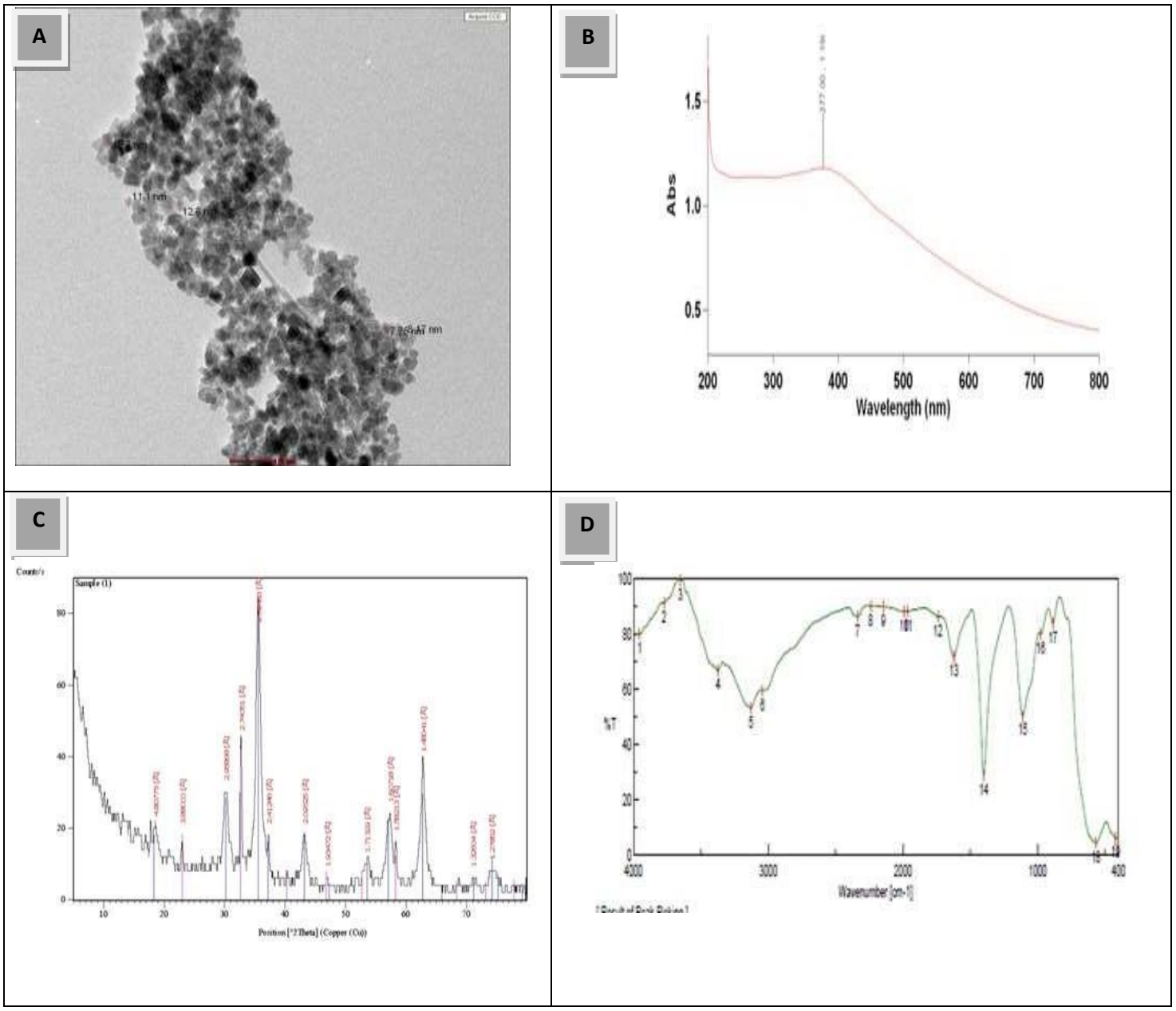

Figure 2 | A) TEM image. B) UV-vis absorption band. C) FTIR spectrum. (D) XRD pattern of magnetite nanoparticles

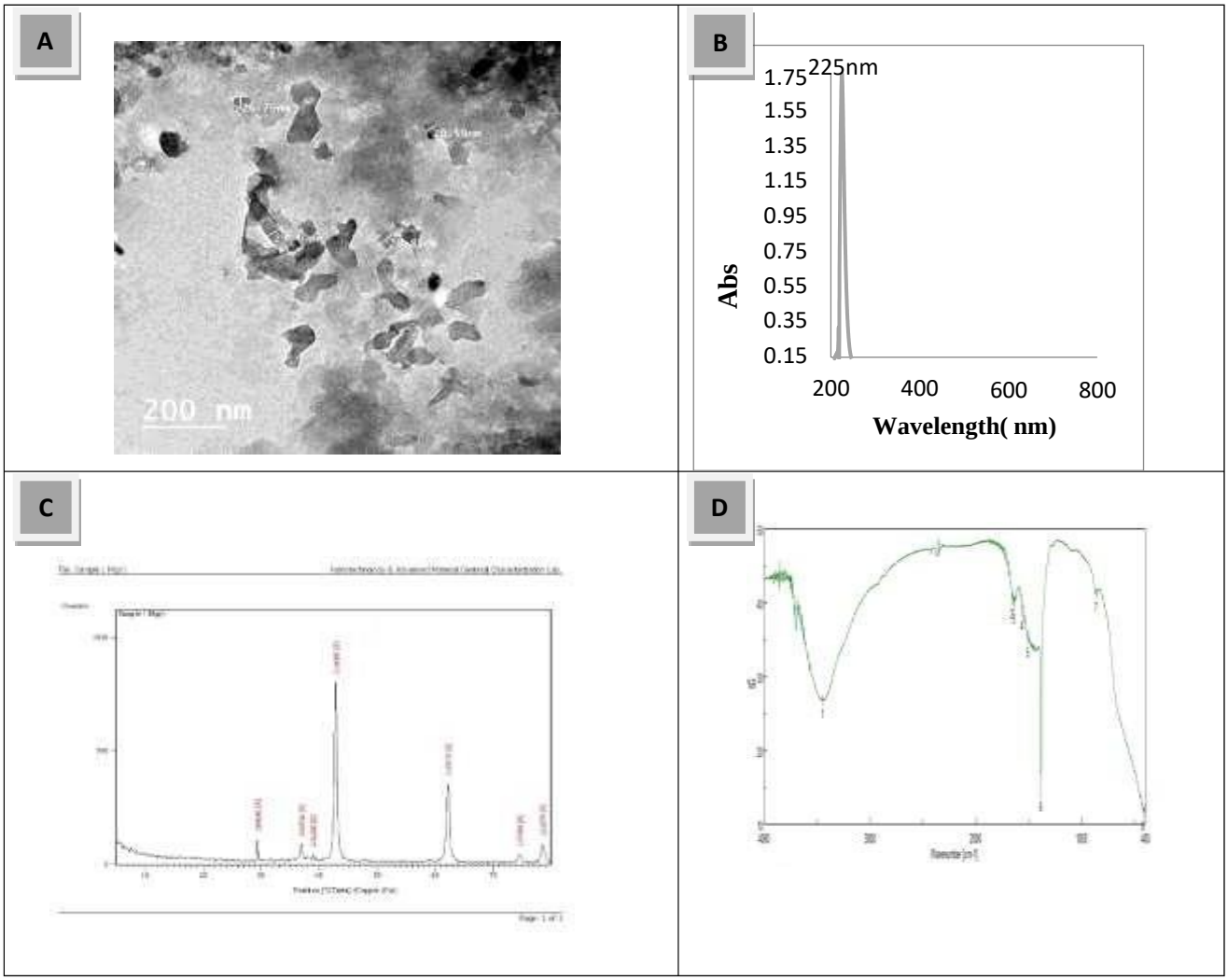

Figure 3 | A) TEM image. B) UV-vis absorption band. C) FTIR spectrum. (D) XRD pattern of MgO nanoparticles

Biological analysis results

Body weight gain in (Figure 4, A) showed that the anemic group had the highest weight gain value among examined groups which has a non-significant effect on the remaining groups except the $FeSO_4$ treated group (the lowest value) on the other hand, feed efficiency ratio (figure 4, C) demonstrated that $FeSO_4$ treated group was the highest value which has a non-significant impact between other groups. However, Figure 4, B showed that the IONPs group had the highest value of feed intake/day (g) 18.03 g, which has a non-significant increasing impact with + ve control (anemic group) and a significant impact with others. Similar observations were found by [35, 64] There was a notable increase in the body weight of all animals during their recovery from anemia, fed with diets of all three formulations. Interestingly, significant body weight gain was observed during the anemia

development stage, as well as during the recovery using all three salt formulations in the diet. There was no influence of a low-iron diet on the body weight of male rats.

Figure 4 (D) illustrated that For Fe intake/day (g) $FeSO_4$ treated group displayed the highest significant value among tested groups which was 0.471 mg Fe / day while there was no - significant impact between the normal (- ve control) group and IONPs group on (0.373, 0.361 mg Fe / day respectively) on the other hand FeMgO-NPs exhibited the lowest value.

Bioavailability indices results group

Results for bioavailability markers revealed that the final HB Fe / day (Fig. 4, E) of + ve control (anemic rats) was the lowest significant value among groups under study to be 9.09 mg which can be due to the lowest HB concentration as a consequence of feeding iron deficiency diet. However, both of $FeSO_4$ and IONPs groups showed a non-significant increase in final HB Fe / day value with each other and with the normal (- ve control) group. Results reflected consequently on the HRE ratio/day % (Figure 4, F) and RBV_{HRE} ratio/day (Figure 4, G), which exhibited that FeMgO-NPs treated group was the highest bioavailability among examined groups which can be seen as 58.831 % of HRE ratio/day % and 4.791% of RBV_{HRE} ratio/day which has non-significant increase with treated groups and normal (-ve control) group. These results are in harmony with Hilty,[16] Who mentioned that the incorporation of Mg into the Fe_2O_3/ZnO) increased the bioavailability from 77% to 91%. This is due to the addition of Mg increased Fe dissolution by Lowering the lattice energy which facilitates dissolution, although enthalpy and entropy of dissolution probably also play a role. However, the anemic group showed significantly lower values than the examined groups. The nanostructured compounds may be as well absorbed as highly bioavailable iron fortificants such as ferrous sulphate, ferrous fumarate and NaFe EDTA (the bioavailability of these three compounds is comparable in non-inhibitory food matrices [16]

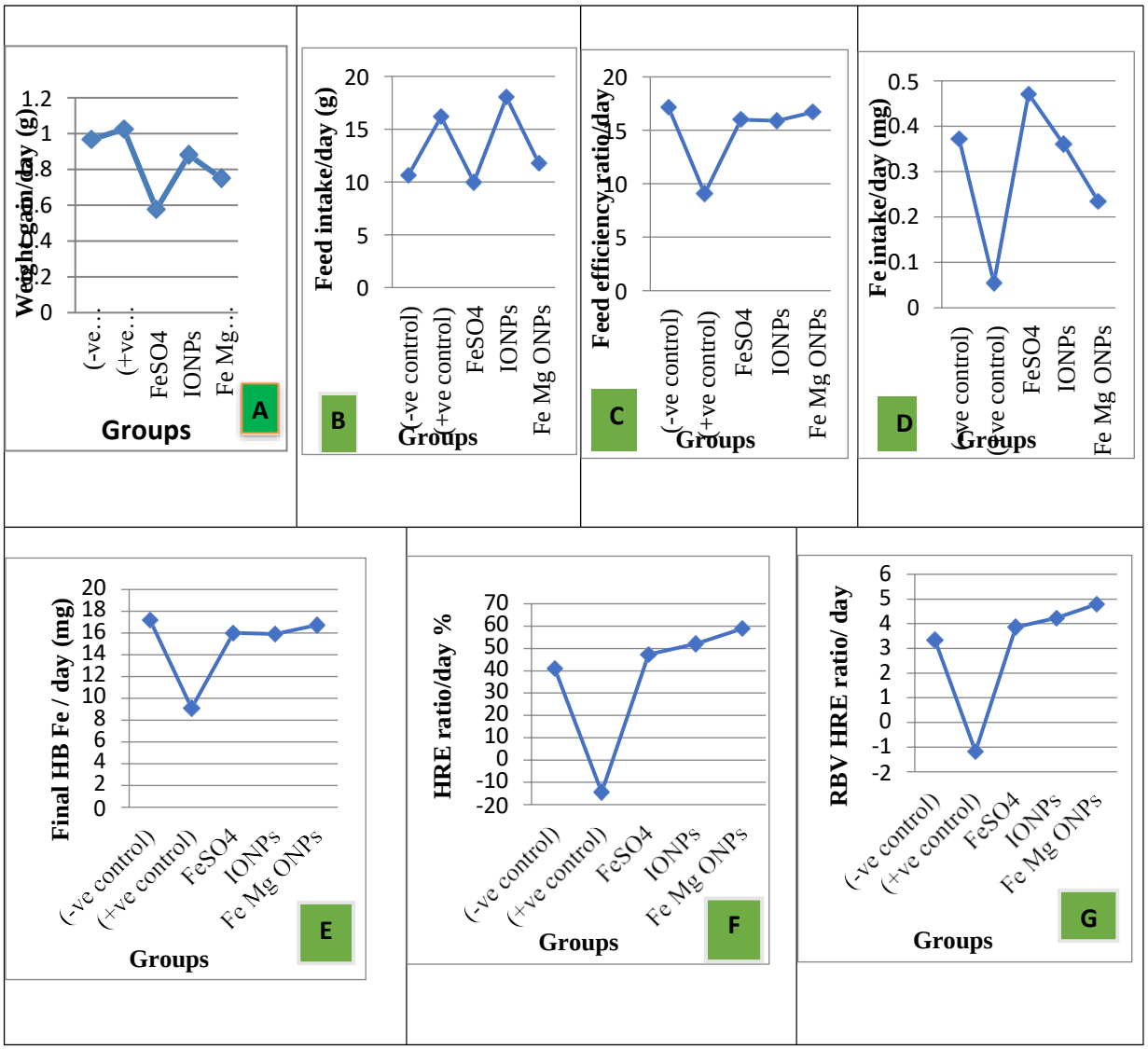

Figure 4 | The biological parameters result and Bioavailability indices A) weight gain/day. B) Feed intake/day. C) feed efficiency ratio/day. D) Fe intake/day (mg). E) Final Initial HB Fe / day (mg). F) HRE ratio /day %. G) RBV $_{HRE}$ ratio /day % in – ve control (normal group), +ve control (anemic group), $FeSO_4$ treated group, Nano Fe treated group and. FeMgO-NPs treated group.

RBC indices results

Analysis of the causes of anemia requires consideration of the whole range of RBC indices and hemoglobin estimation. [65]

According to Table (1) hematological results were explained as follows:

Hemoglobin (Hb) is the main protein in RBCs that is responsible for oxygen transport to different tissues and has a main role in many metabolic processes. So, Hb values were measured to confirm the existence of anemia and to follow up the recovery during the treatment period [66-67]. Results showed that the Fe Mg-ONPs group had the highest value of Hb concentration between examined groups (14.32 g/dl) while +ve control was the lowest one (9.64 g/dl), which verified the induction of microcytic hypochromic anemia. This finding can be due to the effect high iron or zinc intakes can interfere with copper absorption, just as high intakes of divalent metals (copper, calcium, zinc, manganese), which share the same transporter as iron, can interfere with iron absorption and produce iron deficiency [68]. On

the other hand, the anemic rats group treated with IONPs revealed a significant increase compared with +ve control group and non-significant values with $FeSO_4$ treated groups which was seen obviously as 32.05% when compared with +ve control. Low Hb level (<10 g/dL) rats were considered anemic [68]. Other researchers utilized a low-iron diet to induce anemia in the rats for three or eight weeks, resulting in Hb levels of 10 g/dL and 11.9 g/dL, respectively. [70,71]. The anemic group showed a significant decrease in Hb gain values to be (-2.83 g/dl) among examined groups while anemic groups treated otherwise with $FeSO_4$, IONPs, and FeMg-ONPs showed a significant increase in Hb gain level against + ve and -ve control and exhibited a non-significant effect between each other which seen as 3.33g/dl, 2.70 g/dl and 3.47 g/dl for $FeSO_4$, IONPs and FeMgO-NPs treated groups respectively. These results were matched with Hilty et al. [16]

Hematocrit (HCT) values revealed that the anemic group had the significantly lowest values among examined groups giving 28.29 % of HCT and -25.08 % when compared with -ve control while the Fe MgO-NPs treated group exhibited a significantly highest value (40.61 %). However, there was a non-significant increase between Nano Fe and both of -ve control and $FeSO_4$ anemic treated group to give 29.52% when compared with positive control. The remaining results RBC indices (RBC, MCV, MCH) displayed the same manner which observed as + ve control was the lowest values between experimental groups which exhibited as follows 6 10^6/UL of RBC 46,60 of MCV and 15.5 pg MCH while Fe MgO-NPs treated group showed non-significant highest impact with examined groups to be 7.37 10^6/UL, 51.48, 18.74 pg of RBC, MCV, MCH respectively.

Platelet (PLT) results showed a non-significant effect between all examined groups.

White Blood Cell (WBC) results demonstrated that normal control exhibited the highest WBC values with all groups except an anemic group which showed a significant effect with it (the lowest value)

Table (1) Hematological parameters, percent change to negative and positive control of female rats under different experimental treatments

parameters	Normal (Negative control)	Anemic (Positive control)	$FeSO_4$	IONPs	FeMgO-NPs	*P value*
HB (g/dl)	13.43b	9.64 d	12.53 c	12.73 c	14.32 a	0.000
Compared to Negative control %	0.00	-28.22	-6.70	-5.21	6.685	
Compared to Positive control%	39.32	0.00	29.98	32.05	48.597	
HB gain (g/dl)	0.23 b	-2.83c	3.33 a	2.70 a	3.47 a	0.000
Compared to Negative control %	0.00	-1330.4	1347.8	1074	1388.21	
Compared to Positive control%	-108.1	0.00	-217.7	-195.4	-222.56	
HCT %	37.76 b	28.29 d	35.03 c	36.64 bc	40.61 a	0.000
Compared to Negative control %	0.00	-25.08	-7.23	-2.97	7.54	
Compared to Positive control%	33.47	0.00	23.82	29.52	43.53	
RBC (10^6/UL)	7.24 a	6.00 c	7.68 a	7.35a	7.37 a	0.000
Compared to Negative control %	0.00	-17.12	6.13	1.57	1.74	
Compared to Positive control%	20.65	0.00	28.05	22.55	22.75	
MCV	51.07 a	46.60 a	48.00 a	49.90 a	51.48 a	0.077
Compared to Negative control %	0.00	-8.75	-6.01	-2.29	0.809	
Compared to Positive control%	9.59	0.00	3.00	7.08	10.472	
MCH (pg)	18.2a	15.5b	17.4 ab	16.9 ab	18.74 a	0.005
Compared to Negative control %	0.00	-14.84	-4.40	-7.14	3.19	
Compared to Positive control%	17.42	0.00	12.26	9.03	20.60	
WBC (10^3/ul)	14.53 a	8.34 b	12.83 ab	9.62 b	13.14ab	0.015
Compared to Negative control %	0.00	-42.60	-11.70	-33.79	-9.59	
Compared to Positive control%	74.22	0.00	53.84	15.35	57.47	
PLT(10^3/ul)	690.2 a	619 a	648 a	589.8 a	592.6a	0.197
Compared to Negative control %	0.00	-10.32	-6.11	-14.55	-14.14	
Compared to Positive control%	11.50	0.00	4.68	-4.72	-4.26	

Abbreviations: Hb, hemoglobin; HB gain hemoglobin gain; HCT, hematocrit; MCH, mean corpuscular hemoglobin; MCHC, mean corpuscular hemoglobin concentration; MCV, mean corpuscular volume; PLT, platelet; RBC, red blood cell; Ret, reticulocyte; WBC, white blood cell.

Note: *The results were expressed as mean ± SD. ANOVA test was used to compare different markers between the five groups.*

Blood iron saturation analysis

As presented in Fig (5, A), results exhibited that there was a non-significant impact between examined groups while TIBC of anemic rats had the highest value (170.82 µmol/L). On the other hand, the FeMgO-NPs group had the lowest significant value between groups when the remaining groups (Normal group, $FeSO_4$, and IONPs) displayed non-significant values with each other. Serum TIBC in the IDA group was significantly higher than the control group and iron due to progressive Fe depletion from the body stores

[72]. This result reflected on transferrin saturation % as There was a non-significant impact between the IONPs, $FeSO_4$ treated group, and normal control as 61.63 %, 63.28%, and 101.31% respectively. while the FeMgO-NPs group was the highest (173.91 %).

Liver iron content

As illustrated in Figure (5, B), Iron in the liver value of the anemic group was the lowest (122.5 ppm) which decreased by about 88.05 % from the negative control /normal group. Moreover, it has a non-significant effect with the Nano Fe group while $FeSO_4$ treated group was the highest value 1653.2ppm among tested groups. However, the FeMgO-NPs group showed a non-significant increase with the normal group of 1140.6 ppm of iron in the liver and 11.23 % when compared with the negative control. These results were matched with findings of the representative photomicrographs of Prussian blue stained liver sections Fig (6), which exhibited mild positive stainable iron particles in normal and all treated groups except anemic group that exhibited no iron positive particles however, Prussian blue stained spleen Fig (7) sections revealed that normal and the FeMgO-NPs group had moderate positive iron particles but anemic, IONPs and $FeSO_4$ treated group were mild.

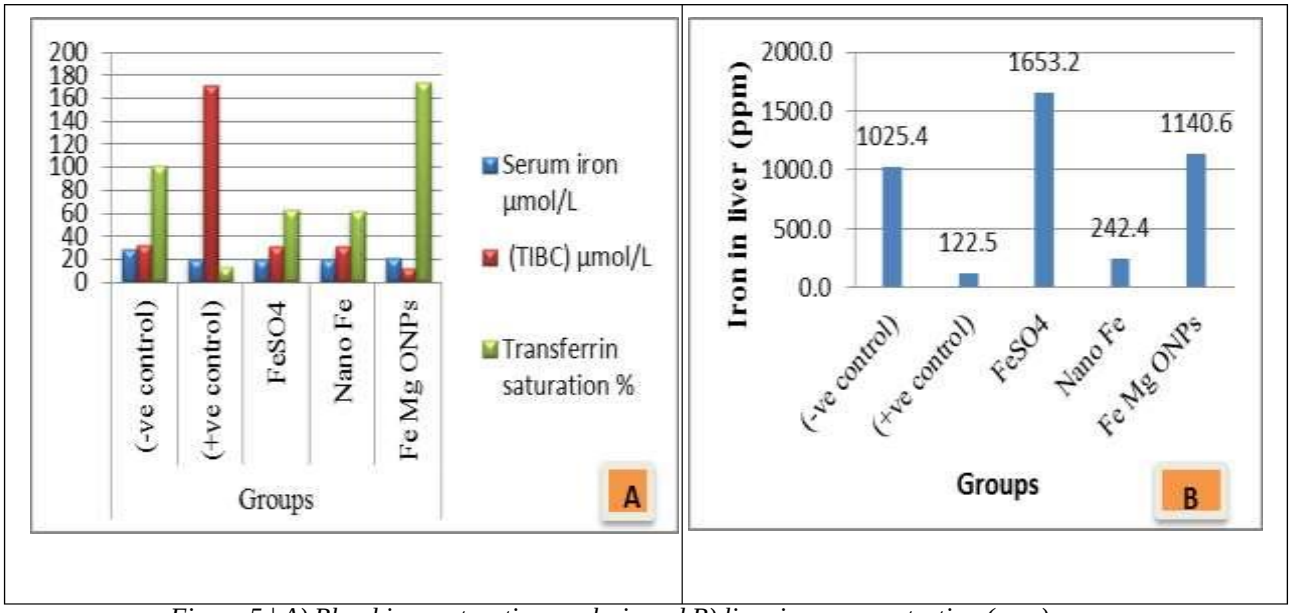

Figure 5 | A) Blood iron saturation analysis and B) liver iron concentration (ppm)

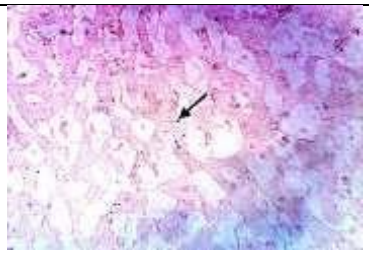 A) Normal group showing mild positive stainable iron particles in the hepatic parenchyma.	 B) Anemic group showing no iron-positive particles.
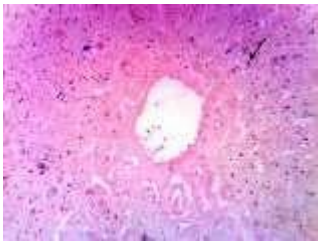 C) $Feso_4$ repleted group showing mild positive stainable iron particles in the hepatic parenchyma.	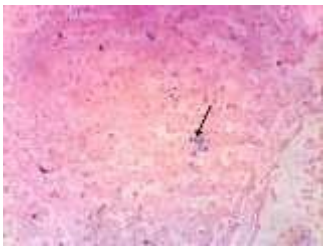 D) IONPs repleted group showing mild positive stainable iron particles in the hepatic parenchyma.
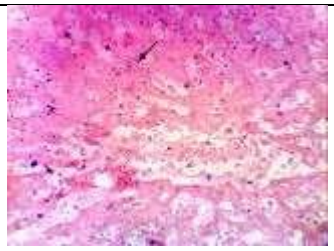 E) Fe Mg ONPs repleted group showing mild positive stainable iron particles in the hepatic	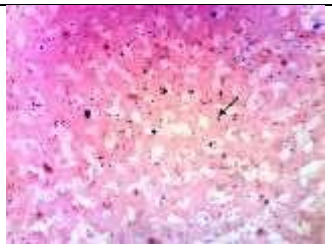 F) Fe Mg ONPs repleted group showing mild positive stainable iron particles in the hepatic

FIGURE 6| (A–H) Representative photomicrographs of Prussian blue stained liver section of rat from the different experimental groups (Prussian blue stain X 400). (A) Normal group (negative control). (B) Anemic group (positive control). (C) Repletion group with FeSO4. (D) Repletion with nano iron. (E, F) FeMgO-NPs

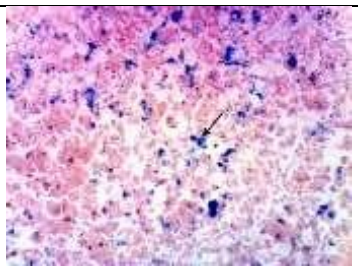 A) Normal group showing moderate positive stainable iron particles.	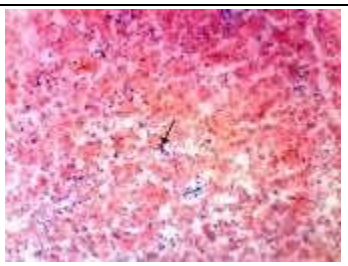 B) Anemic group showing mild positive stainable iron particles
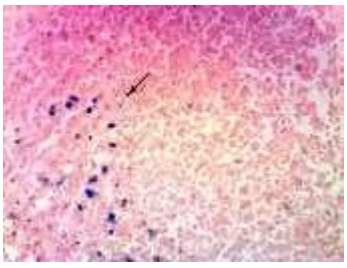 C) $FeSO_4$ repleted group showing mild positive stainable iron particles.	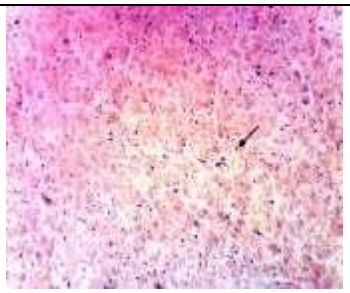 D) IONPs repleted group showing mild positive stainable iron particles
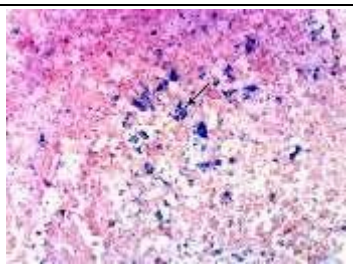 E) FeMgO-NPs repleted group showed moderate positive stainable iron particles**.**	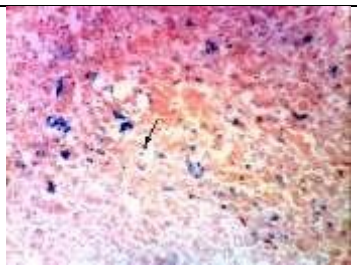 F) FeMgO-NPs repleted group showed moderate positive stainable iron particles**.**

FIGURE 7 | (A–H) Representative photomicrographs of Prussian blue stained spleen sections of rats from the different experimental groups (Prussian blue stain X 400). (A) Normal group (negative control). (B) Anemic group (positive control). (C) Repletion group with $FeSO_4$. (D) Repletion with nano iron. (E, F) Repletion group with FeMgO-NPs.

Histological examination of tissues

The results depicted and illustrated in Figure 8,9 of histopathological examination of the liver and spleen are in line with Feng, et al. [73] who found that when these nanoparticles were incubated in mouse erythrocyte suspension for 4 h at 37 °C, uncoated MNPs (magnetic nanoparticles) displayed severe dose-dependent hemolysis. They further stated that when the dose reaches 2.5 mg/kg or above, acute hemolysis or capillary obstruction can happen as a result of uncoated MNP aggregation, which could cause animal death. [74-75], it was mentioned that because uncoated nanoparticles utilized in biological applications have high surface energy, they can aggregate in blood plasma and cause macrophage absorption by the reticuloendothelial system. Reactive oxygen species production may be aided by the nanostructured materials' large specific surface areas. [76]. The liver specimen exhibited congestion, centrilobular hepatocytes with inflammatory cell infiltration, and perivasculitis, or inflammation of the perivascular sheath and surrounding

tissue. We noticed the typical hepatocyte architecture with central vesicular nuclei emanating from the central vein. When compared to rat control tissue observations, the spleen displayed a decrease in the amount of white pulp. The research also showed that the spleens of iron-deficient rats had decreased hemopoiesis and lymphopoiesis. [73]

<table>
<tr>
<td> 
Fig. (A): Liver of rat from (normal group) showing the normal histological structure of hepatic lobule</td>
<td> 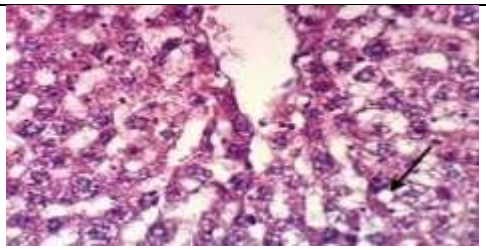
Fig. (B): Liver of rat from (anemic group) showing cytoplasmic vacuolation of hepatocytes.</td>
</tr>
<tr>
<td> 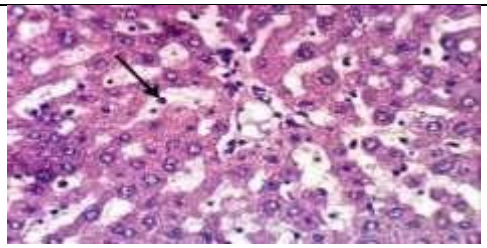
Fig. (C): Liver of rat from (anemic group) showing sinusoidal leukocytosis</td>
<td> 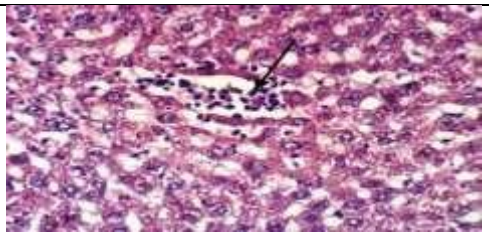
Fig. (D): Liver of rat from (anemic group) showing focal necrosis of hepatocytes associated with mononuclear cell infiltration.</td>
</tr>
<tr>
<td> 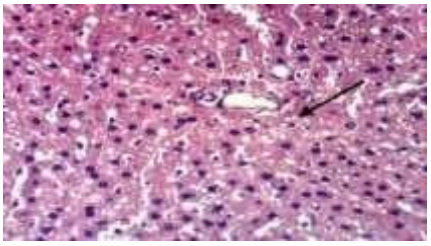
Fig. (E): Liver of rat from (repletion with $Feso_4$) showing cytoplasmic vacuolation of hepatocytes.</td>
<td> 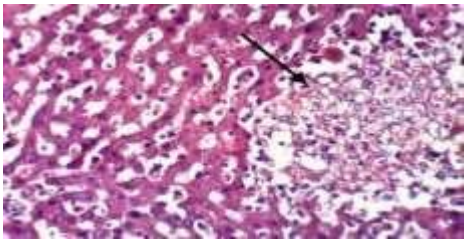
Fig. (F): Liver of rat from (repletion with nano iron) showing focal necrosis of hepatocytes associated with mononuclear cell infiltration.</td>
</tr>
</table>

FIGURE 8| (A–H) Representative photomicrographs of liver sections of rats from the different experimental groups (Hematoxylin and eosin stain X 400). ***(A)*** *Baseline group.* ***(B)*** *Normal group (negative control).* ***(C, D, E)*** *anemic group (positive control).* ***(F)*** *Repletion group with* $Feso_4$. ***(G, H)*** *Repletion with IONPs.* ***(I)*** *Repletion with Fe MgONPs.*

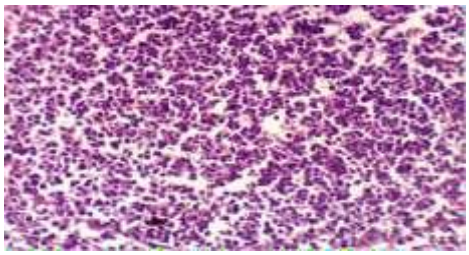

A) Spleen of rat from group normal showing no histopathological changes. Note normal lymphoid follicles

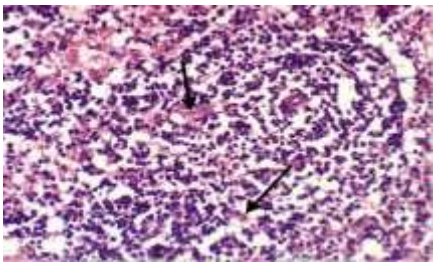

B) Spleen of rat from group anemic showing lymphocytic necrosis replaced by reticular mes

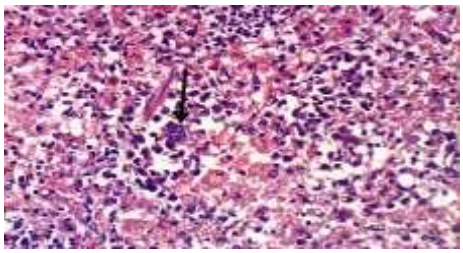

C) Spleen of rat from group anemic showing extramedullary megakaryocytes

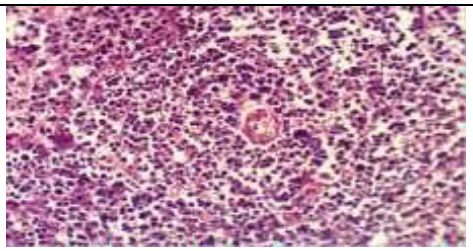

D) Spleen of rat from group repletion with$Feso_4$ showing no histopathological changes

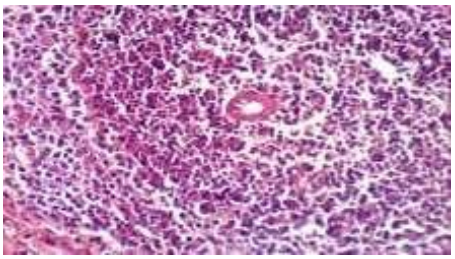

E) Spleen of rat from group repletion with nano i showing no histopathological changes

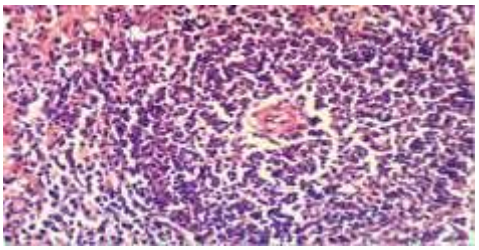

F) Spleen of rat from repleted with FeMg - ONPs showing no histopathological changes.

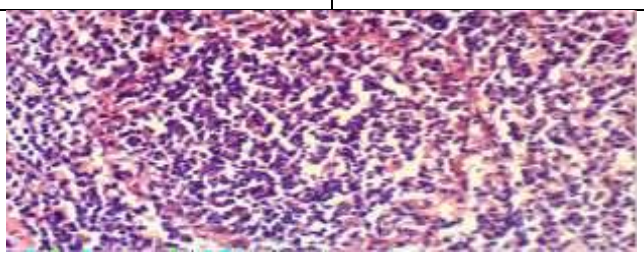

G) Spleen of rat from repleted with Fe MgONPs showing no histopathological changes

FIGURE 9 | (A–H) Representative photomicrographs of Spleen sections of rats from the different experimental groups (Hematoxylin and eosin stain X 400). ***(A)*** *baseline group.* ***(B)*** *Normal group (negative control).* ***(C, D)*** *anemic group (positive control).* ***(E)*** *Repletion group with* $Feso_4$. ***(F)*** *Repletion with nano iron. (G, H) Repletion with FeMgONPs.*

CONCLUSION

Using iron oxide nanoparticles as a food fortifier demonstrated promising bioavailability and hematological results that did not show a significant effect with the traditional iron deficiency anemia treatment source (ferrous sulphate). However, despite these results, there are still some precautions to be taken because it did not relieve the liver tissue damage caused by nutritional iron deficiency anemia, which was resolved by incorporating magnesium with iron. Therefore, we advised researching the long-term management of both IONPs and FeMgO-NPs in iron-deficient anemia.

REFERENCES

1)-Beverina, I. and Ranzini, M., 2023. A synchronized approach between the emergency department and anemia clinic to intravenous iron treatment for very severe (Hb< 7.0 g/dL) and extreme (< 5.0 g/dL) iron-deficiency anemia: short-, medium- and long-term efficacy and safety analysis. *Blood Transfusion*, *21*(3), p.235.

2) - World Health Organization, 2022. WHO Global Anaemia estimates, 2021 Edition. Global anaemia estimates in women of reproductive age, by pregnancy status, and in children aged 6–59 months; 2021. World Health Organization.

3)-Demographic and Health Survey of Egypt 2014.

4)- Obuchowska, A., Standyło, A., Obuchowska, K., Gorczyca, K., Kimber-Trojnar, Ż. and Leszczyńska- Gorzelak, B., 2022. Iron deficiency anemia in pregnancy: evaluation and management. *Journal of Education, Health, and Sport*, *12*(9), pp.168-174.

5)-Miller, W.L., Fudim, M. and Mullan, B.P., 2022. Blood volume and chronic kidney disease in heart failure–Can volume expansion help balance the Cardio-Renal Axis for better clinical outcomes? *Physiological reports*, *10*(23), p.e15526.

6)-Solomon, Y., Gebeyehu, N.A., Adella, G.A., Kassie, G.A., Mengstie, M.A., Seid, M.A., Abebe, E.C., Gesese, M.M., Tegegne, K.D., Anley, D.T. and Zemene, M.A., 2023. Prevalence of anemia and its associated factors among adult asthmatic patients in Northwest Ethiopia. *BMC Pulmonary Medicine*, *23*(1), pp.1-10.

7) - Appiahene, P., Asare, J. W., Donkoh, E. T., Dimauro, G., &Maglietta, R. 2023. Detection of iron deficiency anemia by medical images: a comparative study of machine learning algorithms. BioData Mining, 16(1), 1-20.

8) - WHO.Hemoglobin concentrations for the diagnosis of anemia and assessment of severity.Vitamin and Mineral Nutrition Information System. Geneva: World Health

Organization; 2011. (WHO/NMH/ NHD/MM/11.1) Available at: http://www.who.int/vmnis/indicators/haemoglobin.pdf (accessed May 29, 2018).

9)- Chen, H.; Wu, W.; Tang, S.; Fu, R.; Gong, X.; Hou, H.; Xu, J. Altered fecal microbial and metabolic profile reveals potential mechanisms underlying iron deficiency anemia in pregnant women in China. Bosn. J. Basic Med. Sci. 2022, 22, 923–933

10)- WHO; FAO. Handbook of Nutritionally Essential Mineral Elements, 1st ed.; O'Dell, B.L., Sunde, R.A., Eds.; CRC Press: Boca Raton, FL, USA, 2019; ISBN 978-0-367-40106-1.

11)- Faizo, A. A., Bawazir, A. A., Almashjary, M. N., Hassan, A. M., Qashqari, F. S., Barefah, A. S., ... &Azhar, E. I. 2023. Lack of Evidence on Association between Iron Deficiency and COVID-19 Vaccine-Induced Neutralizing Humoral Immunity. Vaccines, 11(2), 327.

12)- Largueza, C. B. D., Mocellin, M. C., Nunes, J. C., & Ribas, S. A. 2023. Effect of intake of iron-fortified milk on levels of ferritin and hemoglobin in preschoolers: A systematic review and meta-analysis. Clinical Nutrition ESPEN.

13)- Snook, J., Bhala, N., Beales, I.L., Cannings, D., Kightley, C., Logan, R.P., Pritchard, D.M., Sidhu, R., Surgenor, S., Thomas, W. and Verma, A.M., 2021. British Society of Gastroenterology guidelines for the management of iron deficiency anaemia in adults. Gut, 70(11), pp.2030-2051.

14)- Liu, L., Li, Y., Al-Huqail, A. A., Ali, E., Alkhalifah, T., Alturise, F., & Ali, H. E. 2023. Green synthesis of Fe3O4 nanoparticles using Alliaceae waste (Allium sativum) for a sustainable landscape enhancement using support vector regression. Chemosphere, 138638.

15)- Rohner F, Ernst FO, Arnold M, Hilbe M, Biebinger R, Ehrensperger F, Pratsinis SE, Langhans W, Hurrell RF, Zimmermann MB. 2007. Synthesis, characterization, and bioavailability in rats of ferric phosphate nanoparticles. J. Nutr., 137, 614-619.

16)- Hilty FM, Arnold M, Hilbe M, Teleki A, Knijnenburg JTN, Ehrensperger F, Hurrell RF, Pratsinis SE, Langhans W, Zimmermann MB. 2010. Iron from nano compounds containing iron and zinc is highly bioavailable in rats without tissue accumulation. Nat. Nanotechnol., 5, 374-380.

17)- Hilty FM, Knijnenburg JTN, Teleki A, Krumeich F, Hurrell RF, Pratsinis SE & Zimmermann MB. 2011. Incorporation of Mg and Ca into Nanostructured Fe2O3 Improves FeSolubility in Dilute Acid and Sensory Characteristics in Foods. J. Food Sci., 76, N2-N10.

18)- Martín, M., Rodríguez-Nogales, A., Garcés, V., Gálvez, N., Gutiérrez, L., Gálvez, J., Rondón, D., Olivares, M. and Dominguez-Vera, J.M., 2016. Magnetic study on biodistribution and biodegradation of oral magnetic nanostructures in the rat gastrointestinal tract. Nanoscale, 8(32), pp.15041-15047.

19)- Schlachter, E.K., Widmer, H.R., Bregy, A., Lönnfors-Weitzel, T., Vajtai, I., Corazza, N., Bernau, V.J., Weitzel, T., Mordasini, P., Slotboom, J. and Herrmann, G., 2011. Metabolic pathway and distribution of superparamagnetic iron oxide nanoparticles: in vivo study. International journal of nanomedicine, pp.1793-1800.

20)- Chamorro, S., Gutiérrez, L., Vaquero, M.P., Verdoy, D., Salas, G., Luengo, Y., Brenes, A. and Teran, F.J., 2015. Safety assessment of chronic oral exposure to iron oxide nanoparticles. Nanotechnology, 26(20), p.205101.

21)- Zimmermann, M., Rohner, F., Ernst, F., Biebinger, R., Ehrensperger, F., Pratsinis, S. and Hurrell, R., 2007. Synthesis , characterization and bioavailability of ferric phosphate nanoparticles.

22)- Pereira, D.I., Bruggraber, S.F., Faria, N., Poots, L.K., Tagmount, M.A., Aslam, M.F., Frazer, D.M., Vulpe, C.D., Anderson, G.J. and Powell, J.J., 2014. Nanoparticulate iron (III) oxo-hydroxide delivers safe iron that is well absorbed and utilised in humans. Nanomedicine: nanotechnology, biology and medicine, 10(8), pp.1877-1886.

23) -Mohamad Tarhini, Waisudin Badri, Hélène GreigeGerges, Hatem Fessi, Abdelhamid Elaissari, 2021. Developments in Biomedical Engineering and Bioelectronics, Chapter - Nanoparticles/nanoplatforms to carry and deliver the drug molecules to the target site, Pages 249-266

24)- Huang, J., Xu, J., Ye, P. and Xin, X., 2023. Association between magnesium intake and the risk of anemia among adults in the United States. Frontiers in Nutrition, 10, p.1046749

25)- McCreary, P.A., BATTIFORA, H.A., Hahneman, B.M., Laing, G.H., HASS, G.M. and Singh, K., 1967. Leukocytosis, bone marrow hyperplasia and leukemia in chronic magnesium deficiency in the rat. Blood, 29(4), pp.683-690.

26)- Adams, J.B., Sorenson, J.C., Pollard, E.L., Kirby, J.K. and Audhya, T., 2021. Evidence-based recommendations for an optimal prenatal supplement for women in the US, part two: Minerals. Nutrients, 13(6), p.1849.

27)- Biyik, Z., Yavuz, Y.C. and Altintepe, L., 2020. Association between serum magnesium and anemia in patients with chronic kidney disease. International Urology and Nephrology, 52, pp.1935-1941.

28)- Cinar, V., Nizamlioglu, M., Mogulkoc, R. and Baltaci, A.K., 2007. Effects of magnesium supplementation on blood parameters of athletes at rest and after exercise. Biological trace element research, 115, pp.205-212.29)-

29)-Massart, R., 1981. Preparation of aqueous magnetic liquids in alkaline and acidic media. IEEE transactions on magnetics, 17(2), 1247-1248.

30)- Wahab, R., Ansari, S. G., Dar, M. A., Kim, Y. S., & Shin, H. S., 2007. Synthesis of magnesium oxide nanoparticles by sol-gel process. In Materials Science Forum (Vol. 558, pp. 983-986). Trans Tech Publications Ltd.

31)- Parker, H. E ., 1963. Magnesium, calcium, and zinc in animal nutrition. Atomic Absorption Newsletter 2:23.

32)- Reeves, P.G., Nielsen, F.H. and Fahey Jr, G.C., 1993. AIN-93 purified diets for laboratory rodents: final report of the American Institute of Nutrition ad hoc writing committee on the reformulation of the AIN-76A rodent diet. The Journal of nutrition, 123(11), pp.1939-1951.

33)- Yanagisawa, H., Sato, M., Nodera, M., Wada, O., 2004. Excessive zinc intake elevates systemic blood pressure levels in normotensive rats—the potential role of superoxide-induced oxidative stress. J. Hypertens. 22, 543–550.

34)- Yanagisawa, H., Miyakoshi, Y., Kobayashi, K., Sakae, K., Kawasaki, I., Suzuki, Y. and Tamura, J.I., 2009. Long-term intake of a high zinc diet causes iron deficiency anemia accompanied by reticulocytosis and extra-medullary erythropoiesis. Toxicology letters, 191(1), pp.15-19.

35)- Tsao, C. W., Liao, Y. R., Chang, T. C., Liew, Y. F., & Liu, C. Y., 2022. Effects of Iron Supplementation on Testicular Function and Spermatogenesis of Iron-Deficient Rats. Nutrients, 14(10), 2063

36)- Tim K!.Orbital venous anatomy of the rat. Lab AnimSci l979;29: 636-8.

37)- Chapman, D.G., Castillo, R. and Campbell, J.A., 1959. Evaluation of protein in foods: 1. A method for the determination of protein efficiency ratios. Canadian Journal of Biochemistry and Physiology, 37(5), pp.679-686.

38)- Eggum, B.O., 1973.A study of certain factors influencing protein utilization in rats and pigs.Beretn. 406. Fors0gslab. Copenhagen, Denmark, 173 pp.

39)- MAHONEY, A.W. and HENDRICKS, D.G., 1982. Efficiency of hemoglobin regeneration as a method of assessing iron bioavailability in food products.

40)- Forbes, A.L., Arnaud, M.J., Chichester, C.O., Cook, J.D., Harrison, B.N., Hurrell, R.F., Kahn, S.G., Morris, E.R., Tanner, J.T. and Whittaker, P., 1989. Comparison of in vitro, animal, and clinical determinations of iron bioavailability: International Nutritional Anemia Consultative Group Task Force report on iron bioavailability. The American journal of clinical nutrition, 49(2), pp.225-238.

41)- Fritz, J.C., Pla, G.W., Harrison, B.N. and Clark, G.A., 1974. Collaborative study of the rat hemoglobin repletion test for bioavailability of iron. Journal of the Association of Official Analytical Chemists, 57(3), pp.513-517.

42)- Dreux, C., 1977. Selected method. Analysis of human serum: assay of iron II. Method using bathophenanthroline Se-Iron II (bathophenanthroline). In Annales de biologie clinique (Vol. 35, No. 3, pp. 275-277).

43)- Piccardi, G., Nyssen, M., & Dorche, J., 1972. Détermination du fer et de la capacité totale de fixation dans le sérum humain par une méthode sans déprotéinisation. Clinica Chimica Acta, 40(1), 219-228.

44)- Bancroft D, Stevens A, Turner R.: Theory and practice of histological techniques. 4th ed., 1996. Churchill Livingstone, Edinburgh, London, Melbourne

45)- Chan, Y.H., 2003. Biostatistics 102: quantitative data–parametric & non-parametric tests. blood Press, 140(24.08), p.79.

46)- Yadav, B.S., Singh, R., Vishwakarma, A.K. and Kumar, N., 2020. Facile synthesis of substantially magnetic hollow nanospheres of maghemite (γ-Fe_2O_3) originated from magnetite (Fe_3O_4) via solvothermal method. Journal of Superconductivity and Novel Magnetism, 33, pp.2199-2208.

47)- Abbas, I.K. and Adim, K.A., 2023. Synthesis and characterization of magnesium oxide nanoparticles by atmospheric non-thermal plasma jet. Kuwait Journal of Science.

48)-Abinaya, S. and Kavitha, H.P., 2023. Magnesium Oxide Nanoparticles: Effective Antilarvicidal and Antibacterial Agents. ACS omega, 8(6), p.5225

49)- Fathy, M.M., Fahmy, H.M., Balah, A.M., Mohamed, F.F. and Elshemey, W.M., 2019. Magnetic nanoparticles-loaded liposomes as a novel treatment agent for iron deficiency anemia: In vivo study. *Life Sciences*, *234*, p.116787

50)- Winsett, J., Moilanen, A., Paudel, K., Kamali, S., Ding, K., Cribb, W., ...&Neupane, S., 2019. Quantitative determination of magnetite and maghemite in iron oxide nanoparticles using Mössbauer spectroscopy. SN Applied Sciences, 1, 1-8.

51)- Kumar, A., &Gangawane, K. M., 2022.Effect of precipitating agents on the magnetic and structural properties of the synthesized ferrimagnetic nanoparticles by co-precipitation method. Powder Technology, 401, 117298.

52)- Kim, H., Im, P. W., Lee, C., Hong, H., Lee, W., Koo, C., ...&Piao, Y., 2023. In vitro magnetic hyperthermia properties of angle-shaped superparamagnetic iron oxide nanoparticles synthesized by a bromide-assisted polyol method.RSC Advances, 13(5), 2803-2810.

53)-Subash, M., Chandrasekar, M., Panimalar, S., Inmozhi, C., Parasuraman, K., Uthrakumar, R. and Kaviyarasu, K., 2023. Pseudo-first kinetics model of copper doping on the structural, magnetic, and photocatalytic activity of magnesium oxide nanoparticles for energy application. Biomass Conversion and Biorefinery, 13(4), pp.3427-3437.

54)-Ameur, I., Khantoul, A.R., Boudine, B., Brien, V., Horwat, D., Sebais, M. and Halimi, O., 2023. Effects of Erbium Incorporation on Structural, Surface Morphology, and Degradation of Methylene Blue Dye of Magnesium Oxide Nanoparticles. Journal of Inorganic and Organometallic Polymers and Materials, 33(1), pp.30-46.

55) - Budnevsky, A.V., Voronina, E.V., Ovsyannikov, E.S., Tsvetikova, L.N., Zhusina, Y.G. and Labzhaniya, N.B., 2017. Anemia of chronic diseases as a systemic manifestation of chronic pulmonary obstructive disease. Klinicheskaia Meditsina, 95(3), pp.201-206.

56)- Li, Y.Q., Fu, S.Y. and Mai, Y.W., 2006. Preparation and characterization of transparent ZnO/epoxy nanocomposites with high-UV shielding efficiency. Polymer, 47(6), pp.2127-2132.

57) - Zhang, Y., Wang, Q., Cheng, J., Zhang, J., Xu, J. and Ren, Y., 2015. Comprehensive profiling of mercapturic acid metabolites from dietary acrylamide as short-term exposure biomarkers for evaluation of toxicokinetic in rats and daily internal exposure in humans using isotope dilution ultra-high performance liquid chromatography-tandem mass spectrometry. Analytica chemical acta, 894, pp.54-64.

58) - Pachiyappan, J., Gnanansundaram, N., Sivamani, S., Sankari, N.P.B.P., Senthilnathan, N. and Kerga, G.A., 2022. Preparation and characterization of magnesium oxide nanoparticles and their application for photocatalytic removal of rhodamine B and methylene blue dyes. Journal of Nanomaterials.

59)- Nga, N.K., Chau, N.T.T. and Viet, P.H., 2020. Preparation and characterization of a chitosan/MgO composite for the effective removal of reactive blue 19 dye from aqueous solution. Journal of Science: Advanced Materials and Devices, 5(1), pp.65-72.

60)- Barzegar, M., Ahmadvand, D., Sabouri, Z. and Darroudi, M., 2023. Green synthesis of magnesium oxide nanoparticles by chitosan polymer and assessment of their photocatalytic activity and cytotoxicity influences. Materials Chemistry and Physics, 301, p.127649

61)- Behera, S.S., Patra, J.K., Pramanik, K., Panda, N. and Thatoi, H., 2012. Characterization and evaluation of antibacterial activities of chemically synthesized iron oxide nanoparticles.

62)-Rajalakshmi, A., Ramesh, M., Divya, E., Kavitha, K., Puvanakrishnan, R. and Ramesh, B., 2022. Production and characterization of naturally occurring antibacterial magnetite nanoparticles from magneto-tactic Bacillus sp. MTB17. *Journal of Applied Microbiology*, *132*(4), pp.2683-2693.

63)-Todan, L., Predoană, L., Petcu, G., Preda, S., Culiță, D.C., Băran, A., Trușcă, R.D., Surdu, V.A., Vasile, B.Ș. and Ianculescu, A.C., 2023. Comparative Study of MgO Nanopowders Prepared by Different Chemical Methods. Gels, 9(8), p.624.

64)- Susanti, T., Dirgahayu, P. and Indarto, D., 2017, December. Development of rat model with iron deficiency anemia by modification of its standard food. In 2nd Public Health International Conference (PHICo 2017) (pp. 107-110). Atlantis Press.

65)-Hosseinpour, M., Hatamnejad, M.R., Montazeri, M.N., Akbari Khezrabadi, A., Shojaeefard, E. and Khanzadeh, S., 2022. Comparison of the red blood cell indices based on accuracy, sensitivity, and specificity to predict one-year mortality in heart failure patients. *BMC Cardiovascular Disorders*, *22*(1), pp.1-13.

66)- Enakaya, N.A., Jefferson, A., Chew-Martinez, D. and Matthews, J.S., 2023. Design, Synthesis, and Evaluation of Allosteric Effectors for Hemoglobin. *Accounts of Chemical Research*, *56*(11), pp.1279-1286.

67)-Kaur, L., Singh, A., Datta, A. and Ojha, H., 2023. Multispectroscopic studies of binding interaction of phosmet with bovine hemoglobin. *Spectrochimica Acta Part A: Molecular and Biomolecular Spectroscopy*, *296*, p.122630.

68)-Kaur, R., Mishra, S., Nevolin, I. V., Choudhury, D. R., & Singh, M., 2022. Nutritional anemia: Patent landscape. World Patent Information, 70, 102123.

69)-Shinde, D.B., Koratkar, S.S., Rale, V., Nm, S. and Mishra, N., 2022. Effect of Encapsulated Ferrous Sulphate Fortified Salt on Hemoglobin Levels in Anemic Rats. *Foods*, *11*(12), p.1795.

70)-Xiao, C., Lei, X., Wang, Q., Du, Z., Jiang, L., Chen, S., ...&Ren, F., 2016. Effects of a tripeptide iron on iron-deficiency anemia in rats. Biological trace element research, 169, 211-217.

71)-Zhu, Q., Qian, Y., Yang, Y., Wu, W., Xie, J., & Wei, D., 2016. Effects of carbonyl iron powder on iron deficiency anemia and its sub-chronic toxicity. journal of food and drug analysis, 24(4), 746-753.

72)- Thakur, M. K., Kulkarni, S. S., Mohanty, N., Kadam, N. N., & Swain, N. S., 2019. Standardization and development of rat model with iron deficiency anemia utilizing commercially available iron-deficient food. Biosciences Biotechnology Research Asia, 16(1), 71.

73)- Feng, Q., Liu, Y., Huang, J., Chen, K., Huang, J., & Xiao, K., 2018.Uptake, distribution, clearance, and toxicity of iron oxide nanoparticles with different sizes and coatings. Scientific reports, 8(1), 1-13.

74)- Raynal, I., Prigent, P., Peyramaure, S., Najid, A., Rebuzzi, C. and Corot, C., 2004. Macrophage endocytosis of superparamagnetic iron oxide nanoparticles: mechanisms and comparison of ferumoxides and ferumoxtran-10. Investigative radiology, 39(1), pp.56-63.

75)- Rogers, W.J. and Basu, P., 2005. Factors regulating macrophage endocytosis of nanoparticles: implications for targeted magnetic resonance plaque imaging. Atherosclerosis, 178(1), pp.67-73.

76)- Auffan, M., Achouak, W., Rose, J., Roncato, M.A., Chaneac, C., Waite, D.T., Masion, A., Woicik, J.C., Wiesner, M.R. and Bottero, J.Y., 2008. Relation between the redox state of iron-based nanoparticles and their cytotoxicity toward Escherichia coli. *Environmental Science & Technology*, *42*(17), pp.6730-6735.